Low-Energy Continuous X-Ray Spectrum in the 80 A to 180 A Region*

T. J. PETERSON, JR., AND D. H. TOMBOULIAN
Department of Physics, Laboratory of Atomic and Solid State Physics, Cornell University, Ithaca, New York
(Received August 7, 1961)

The paper deals with the relative intensity measurements of the soft x-ray continuous radiation from Mg, Al, Mn, Cu, Ge, and Ag targets bombarded by low-energy electrons. The investigations lie in the heretofore unexamined region from 80 to 180 A. Photometric measurements were carried out by the use of a previously calibrated grazing incidence spectrograph. In all cases the target layers were prepared by deposition in high vacuum. Accelerating potentials ranged from 600 to 3000 v. In addition to the study of the spectral shape of the bremsstrahlung, attempts were made to investigate the dependence of the intensity on takeoff angle. Various factors which might modify the source distribution are considered. For incident electrons in the above-mentioned range, the observed intensity at a wavelength λ can be represented by a functional form such as $1/\lambda^{\alpha}$, where the parameter α is found to be in the range from 1.8 to 2.7. This parameter is related to the accelerating potential, the atomic number, and ν/ν_0, where ν is the radiated frequency and ν_0 is the high-frequency limit. In the cases of Mg and Mn where the incident electron energies were of the order of 600 ev, comparison reveals that the observations are in agreement with numerical presentations of the Sommerfeld thin-target theory which assumes one radiating interaction between the incident electron and a single layer of target atoms.

I. INTRODUCTION

THERE appears to be a limited amount of experimental data on the very low energy continuous x-ray spectrum, particularly in the 100-A wavelength region. Therefore an investigation was undertaken to examine the continuum in this spectral region. The study was facilitated by the availability of a grazing incidence spectrograph[1] which was calibrated over the 80-A to 180-A interval. The experiments involved a measurement of the relative intensity and its dependence on accelerating potential, target material, and angle of observation. Portions of these results have already been presented in preliminary reports.[2]

Duane and Hunt[3] established the existence of a cutoff frequency given by $\nu_{\max}=eV/h$, where V is the accelerating voltage. Almost all reported work on the continuous x-ray spectrum at energies below 5 kev has been aimed at investigations of the spectrum close to the Duane-Hunt limit.[4] Stephenson and Mason[5] have reported upon the continuous spectrum from tungsten at wavelengths extending from 8 to 14 A and at target voltages ranging from 1.1 to 2.0 kv. In the interval 6 to 20 A, Neff[6] has presented measurements of the continuous radiation from a platinum target at selected potentials in nearly the same voltage range. The aforementioned investigations represent the available information at wavelengths extending to about 20 A. On the theoretical side, there are extensive studies of the bremsstrahlung produced by high-energy electrons,[7] but, as shall be pointed out subsequently, only the numerical presentation of the basic Sommerfeld theory[8] by Kirkpatrick and Wiedmann[9] is particularly applicable to the case of very low-energy nonrelativistic electrons as dealt with here.

II. EXPERIMENTAL

The x-ray source was a four-sided, rotatable stainless steel target. It was mounted in a glass x-ray tube along with an electron source and evaporation assembly. The element to be studied was evaporated onto the target surface just prior to exposure so that emission was observed only from fresh surfaces within 1 hr of deposition. This target layer was more than 400 A thick in all cases so that all the incident electrons were stopped within the deposited layer. The spectra were recorded photographically by means of a grazing incidence vacuum spectrograph in which the dispersing element was a lightly ruled concave glass grating having 30 000 lines/in. and a radius of 154 cm. The radiation was incident at a grazing angle of 4.64°. Further details regarding the instrumental arrangements may be found in the survey article[10] by one of the authors. The x-ray tube filament was centered in front of the target face at a distance of 3 mm. The takeoff angle θ was limited by tube geometry and its range was 95°–135°. (The angle θ is defined to be the angle between the normal *into* the target surface and the direction of photon observation as defined by the line from the center of the target face to the center of the grating.) Values of θ which are slightly greater than 90° represent observations of the spectrum at a grazing angle with respect to the target face.

* The research was supported in part by the U. S. Army Research Office (Durham).

[1] G. Sprague, D. H. Tomboulian, and D. E. Bedo, J. Opt. Soc. Am. **45**, 756 (1955).

[2] T. J. Peterson, Jr. and D. H. Tomboulian, Bull. Am. Phys. Soc. **4**, 263 (1959); **4**, 419 (1959); **6**, 284 (1961).

[3] W. Duane and F. L. Hunt, Phys. Rev. **6**, 166 (1915).

[4] See the survey articles by H. Kulenkampff in *Handbuch der Physik* edited by H. Geiger and K. Scheel (Verlag Julius Springer, Berlin, 1933) Vol. 23/2, p. 142; or, more recently S. T. Stephenson in *Handbuch der Physik*, edited by S. Flügge (Springer-Verlag, Berlin, 1957), Vol. 30, p. 357.

[5] S. T. Stephenson and F. D. Mason, Phys. Rev. **75**, 1711 (1949).

[6] H. Neff, Z. Physik **131**, 1 (1951).

[7] H. W. Koch and J. W. Motz, Revs. Modern Phys. **31**, 920 (1959).

[8] A. Sommerfeld, *Atombau und Spektrallinien* (Vieweg und Sohn, Braunschweig, 1939), 2nd ed., Vol. 2, p. 495.

[9] P. Kirkpatrick and L. Wiedmann, Phys. Rev. **67**, 321 (1945). See also J. M. Berger, *ibid.* **105**, 35 (1957) for more recent calculations of portions of the problem.

[10] D. H. Tomboulian, in *Handbuch der Physik*, edited by S. Flügge (Springer-Verlag, Berlin, 1957), Vol. 30, p. 246.

At a given position on the Rowland circle, radiation of wavelengths λ_1, $\lambda_1/2$, $\lambda_1/3$, . . . will be brought to a focus, provided the particular wavelength is present in the source and is reflected by the grating. The amount of radiation diffracted into a wavelength band $d\lambda_1$ centered at λ_1 is a small fraction of that which is incident upon the grating. This fraction must be known for every wavelength involved in order to obtain the spectral distribution of the source from observations. The conversion procedure has been described in an earlier paper.[11] The properties of the grating and the particular angle of incidence were such that radiation of wavelength less than 90A was not significantly reflected in the second order, therefore the spectrum at wavelengths shorter than 180A was free from order overlap. This grating response had been calculated[1] and indirectly confirmed[11] by previous work.

The target potential ranged from 600 to 3000 v and the tube current was fixed at 200 ma. This current was stabilized by means of an electronic regulating circuit which controlled the filament heating current in response to fluctuations in the target current. Observations indicated that the tube current became space-charge limited and dropped rapidly as the accelerating potential difference was reduced below 500 v, necessitating a corresponding increase in exposure time. The instrumental limitations on observations at wavelengths shorter than 80 A precluded studies of the spectrum near the Duane-Hunt limit.[12] Ilford Q1 emulsion on thin glass plates was used exclusively. Available information[11] indicates that in the 100-A region this emulsion has a response which is flat in energy. Exposure times of 3–9 hr were required to produce blackening satisfactory for photometry. Operating pressures in the x-ray tube were of the order of 1×10^{-6} mm of mercury.

In the treatment of data, the dependence of the relative intensity on wavelength is deduced by photometric reduction. The numerical result at a given wavelength depends upon factors such as target atomic number, power input, takeoff angle, and exposure. To facilitate comparison, a normalization of $I(\lambda)$, the observed relative intensity per unit wavelength interval, was carried out. Examination of the data indicated that a plot of $\log I(\lambda)$ as a function of $\log\lambda$ yielded a nearly straight line; therefore, it seemed reasonable to approximate $I(\lambda)$ by a function of the type B/λ^α, where α and B are adjustable parameters. As the first step in this procedure, the logarithmic plot was constructed and the best value of α obtained from it. Then B was chosen so that $B/80^\alpha=100$; i.e., the approximation function for the relative intensity was fixed at 80 A. A least-squares fit between the data and the B/λ^α curve

[11] D. H. Tomboulian and P. L. Hartman, Phys. Rev. **102**, 1423 (1956).

[12] For this limit to be in excess of 80A, the accelerating potential must be less than 155 v. Such low potentials require inordinately long exposures.

TABLE I. Normalized values of $I(\lambda)$ at a target potential of 3.0 kv for a takeoff angle of 110°.

Wavelength in angstroms	Relative intensities Al	Mn	Cu	Ge	Ag
80	102	101	101		99.0
85	96.7	91.8	90.7		87.6
90		82.5			81.7
95	79.1	72.4	68.4		71.0
100	65.2	60.8	57.6		59.5
105	59.8	58.2	53.1		53.7
110	52.6	51.7	47.0		46.9
114	49.1	49.9	45.7		43.9
120	44.6	42.2	39.0		37.3
125	42.5	39.3	36.9		30.8
130		37.3	35.1		25.0
135		35.3			22.7
140		32.2			19.8
145		28.7		21.6	17.3
150		25.5		18.9	16.1
155		23.2		16.8	15.0
160		21.2		15.2	14.6
165		19.5		13.6	13.6
170		17.6		12.6	12.6
175		17.0		11.8	12.1
180		16.3		11.0	11.4
α:	1.8	2.1	2.2	2.7	2.7

was obtained by finding a multiplicative constant c for $I(\lambda)$ so that D, defined by

$$D=\sum_{\lambda=80,90,100,\ldots}^{\lambda=180}\left\{\frac{B}{\lambda^\alpha}-cI(\lambda)\right\}^2, \tag{1}$$

is a minimum. Of course, D could have been calculated for discrete wavelengths at intervals less than 10 A, but the chosen interval proved satisfactory for the purpose. The value of c which makes D a minimum is

$$c=\sum_{\lambda=80,90,100,\ldots}^{\lambda=180}\frac{B}{\lambda^\alpha}I(\lambda)\Big/\sum_{\lambda=80,90,100,\ldots}^{\lambda=180}\{I(\lambda)\}^2. \tag{2}$$

The observed values of $I(\lambda)$ were multiplied by c to produce a new sequence ranging from approximately 100 at $\lambda=80$ A to values between 30 and 10 at $\lambda=180$ A. These values were used to plot the experimental curves.

III. RESULTS AND DISCUSSION

1. Measurements on Al, Mn, Cu, Ge, and Ag at 3 kv and a Takeoff Angle of 110°

Observations of the continuous spectrum belonging to the above listed elements were conducted under the specified operating conditions. The normalized values of $I(\lambda)$ are listed in Table I. Omitted entries in the tables occur at wavelength bands where it was not feasible to isolate the continuum from the overlying characteristic emission bands. The only significant contaminating radiation observed was the carbon K band which in the first order covers[13] a wavelength span

[13] F. C. Chalkin, Proc. Roy. Soc. (London) **A194**, 42 (1948).

of 2.5A centered at 44.8A. This first-order emission was observable in the spectrograph since the short-wavelength cutoff of the grating occurred at 40 A. The peak intensity in this emission band was typically around three times the continuum intensity at 44.8 A. This intense radiation also appeared in the second order at 89.6A and weakly in the third order. In this respect, the behavior of the carbon line is anomalous. For significantly less intense radiation, the grating response is such that we can still regard the continuum as free from overlap in the region of interest.[1] A characteristic dip which originates from absorption in the grating blank was observed in the wavelength region from 114 to 118 A for every run.

The source distribution is modified primarily by self-absorption in the target, by the instrumental window, by the response of the grating and that of the detector. The self-absorption problem will be discussed in a following section. The term instrumental window refers to the broadening of a very narrow band of source frequencies into an infinite distribution of frequencies at the detector. This latter distribution has an apparent finite width which may be studied by analysis of the observed intensity distribution of a single atomic spectral line. The instrumental line shape was found to be well represented by a Gaussian distribution with full width at half-maximum of the order of 0.6 A. Mathematically, the effect of the window function can be stated as

$$O(E)=\int_{-\infty}^{\infty} S(E')W(E,E')dE', \tag{3}$$

where $O(E)$ represents the observed distribution, $S(E')$ the source distribution, and $W(E,E')$ the instrumental window function, which is normalized so that

$$\int_{-\infty}^{\infty} W(E')dE'=1. \tag{4}$$

A $1/\lambda^2$ dependence of the relative intensity per unit wavelength interval corresponds to constant relative intensity per unit energy interval. If $S(E)$ is independent of E over a finite range, then the window function in this special case of $\alpha=2$ gives an $O(E)$ which has the same shape as $S(E)$. Since the preceding argument is not applicable to the case where $\alpha\neq 2$, a short graphical method given by Bracewell[14] was used to estimate the effect of the experimental window in the case where $\alpha=3$. This treatment produces negligible correction to the observed spectrum, in accordance with his observations and general experience that the effect of window is most important for spectra which exhibit sharp variations in intensity over narrow ranges. The procedures for dealing with the grating response and the arguments in favor of the flat response of the emulsion have been referred to earlier. The photometric reduction also involves problems connected with reflection at the emulsion surface and preferential absorption by the emulsion. The instrumental arrangement is such that 80-A photons are incident upon the plate at a grazing angle of 9.14° while 180 A photons strike at an angle of 12.7°. The fraction of energy incident upon the plate which is lost by reflection is assumed to be constant over this limited range of angles. From emission band studies[15] of silver bromide its M absorption edge is deduced to be at 190 A and falls beyond the range covered in this work.

For the elements listed in the subheading, the values of α which provide the best fit between the data and the approximation function B/λ^{α} are indicated in Table I. The intensity distribution in the continuous x-ray spectrum from a thick target had been given empirically by Kulenkampff[16]:

$$I(\lambda)=(cZ/\lambda^2)[(1/\lambda_0-1/\lambda)+bZ]. \tag{5}$$

Relation (5) for $\lambda\gg\lambda_0$ reduces essentially to a $1/\lambda^2$ dependence. The current results indicate that this relation does not hold in the range of energies and wavelengths specified herein.

TABLE II. Normalized values of $I(\lambda)$ at various target potentials for a takeoff angle of 110°.

Wavelength in angstroms \ Target potential in kv	3.0	1.5	1.0	0.5	3.0	1.2
	Silver				Manganese	
80	99.0	99.0	99.7		101.5	100.1
85	87.6	92.2	98.7		91.8	91.2
90	81.7				82.5	81.3
95	71.0	76.6	80.6	74.9	72.4	70.8
100	59.5	64.5	64.3	65.9	60.8	62.1
105	53.7	60.1	61.2	62.8	58.2	60.5
110	46.9	52.9	55.6	56.6	50.8	53.6
114	43.9	50.2	52.7	55.9	49.9	52.9
120	37.3	45.3	43.4	47.9	42.2	45.0
125	30.8	38.8	43.2	44.8	39.3	43.6
130	25.0	35.4	41.0	41.1	37.3	41.2
135	22.7	32.4	38.0	37.9	35.3	39.2
140	19.8	29.5	31.0	33.2	32.2	35.1
145	17.3	25.7	26.0	28.1	28.7	32.3
150	16.1	22.3	23.9	25.2	25.5	29.6
155	15.0	20.9	21.0	22.2	23.2	26.8
160	14.6	19.1	19.0	19.8	21.2	23.6
165	13.6	16.9	17.8	18.5	19.5	21.6
170	12.6	17.2	16.2	18.2	17.6	20.1
175	12.1		16.1	16.8	17.0	18.2
180	11.4			16.3	16.3	17.4
α:	2.7	2.4	2.4	2.2	2.2	2.1

2. Data on Ag and Mn at Various Potentials for a Fixed Takeoff Angle of 110°

Both Ag and Mn serve as excellent target materials for the study of bremsstrahlung between 80 and 180 A

[14] R. N. Bracewell, J. Opt. Soc. Am. **45**, 873 (1955).

[15] H. M. O'Bryan and H. W. B. Skinner, Proc. Roy. Soc. (London) **A176**, 229 (1940).

[16] H. Kulenkampff, Ann. Physik. **69**, 548 (1922).

because the spectra are free from the presence of emission bands characteristic of the elements themselves. Consequently, observations with Ag and Mn were made at various lower potentials. These measurements provide information about the spectrum closer to the short-wavelength cutoff since the wavelength range attainable by the spectrograph is limited. An analysis of the data in Table II indicates that α decreases with increasingly lower accelerating potentials.

3. Spectral Dependence on Takeoff Angle

When a bombarding electron interacts with the Coulomb field of a single unshielded nucleus, it will emit a photon. The Sommerfeld theory[8] provides probabilities that this energy will lie in some specified range and that the photon will be emitted in some particular direction. This theory has been developed only for a "thin" target wherein each electron has only one radiating interaction with a single layer of atoms. The mathematical result is not in a simple closed form. The problem of predicting the source distribution is laborious. Kirkpatrick and Wiedmann[9] have carried out the calculations and have provided intensity curves as functions of V/Z^2 and ν/ν_0, where ν_0 is the cutoff frequency. Taking the x axis as the direction of incident electron velocity, the observed intensity at an angle θ (as previously defined) is given in terms of the intensity components I_x and I_y by the expression[9]

$$I(\theta)=I_x\sin^2\theta+I_y(1+\cos^2\theta). \quad (6)$$

The magnitude of the angular dependence in the case of Mg at $V=675$ v is shown in Table III. This table contains results evaluated by the use of Eq. (6) as well as those from experiment. Within the spread (see Fig. 1) of the data, no definite conclusion can be drawn as to the effect of the takeoff angle. Additional observations of this nature were carried out for Mn and Ag (see Table IV). Though these measurements fall outside the range of the Kirkpatrick and Wiedmann calculations, they still indicate that with increasing θ the relative intensity increases at longer wavelengths in harmony with the general behavior predicted by Eq. (6).

TABLE III. Theoretical and experimental values of $I(\lambda)$ from a Mg target at various takeoff angles.

Wavelength in angstroms \ θ:	Relative intensities 95° Theory	95° Experiment	110° Theory	110° Experiment	135° Theory	135° Experiment
80	100	101	100	105	100	117
85	89.2	91.2	89.7	95.7	90.5	105
90	80.0	82.2	80.7	86.3	82.1	95.0
95	72.9	70.4	73.7	75.9	75.5	78.2
100	66.2	61.6	67.2	63.5	69.2	64.6
105	60.8	56.2	61.8	59.3	63.9	57.0
110	55.3	51.1	56.4	53.3	58.6	52.0
114	52.0	49.8	53.1	51.0	55.3	50.5
120	47.0	45.3	48.1	44.1	50.2	42.9
125	42.8	43.0	43.9	43.5	46.0	42.6
130	40.0	40.8	41.1	41.2	43.2	40.8
135	37.5	39.3	38.6	39.4	40.8	38.6
140	35.0	37.2	36.1	36.8	38.3	36.8
145	33.0	33.6	34.1	33.7	36.2	33.5
150	30.8	30.5	31.9	30.0	34.0	30.4
155	29.0	27.9	30.0	27.7	32.1	27.1
160	26.8	25.7	27.8	25.2	29.9	24.9
165	25.0	23.6	26.0	23.4	28.1	23.7
170	23.5	22.6	24.5	22.3	26.5	23.0
175	22.2	21.6	23.2	21.6	25.2	21.9
180	20.5	21.1	21.5	20.8	23.4	21.4

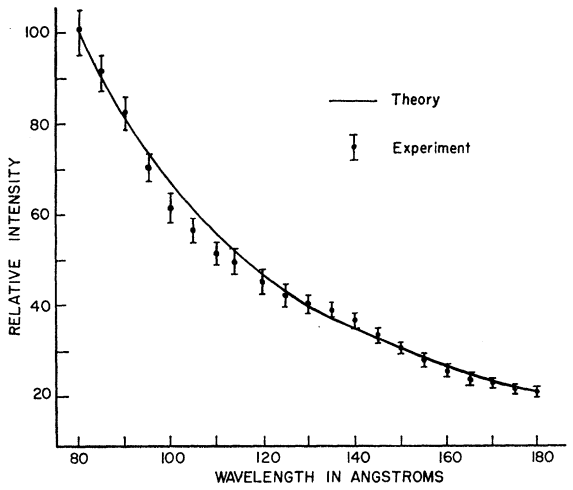

FIG. 1. Comparison of theory with measurement. Mg target at 675 v and at a takeoff angle of 95°. The vertical bars designate the spread in the intensity determinations at the selected wavelengths.

TABLE IV. Normalized values of $I(\lambda)$ at selected target potentials and takeoff angles.

Wavelength in angstroms \ θ: / Target potential kv:	Relative intensities Manganese 95° 1.2	Manganese 110° 1.2	Silver 95° 1.5	Silver 110° 1.5
80	99.4	100.1	100.4	99.0
85	89.8	91.2	87.3	92.2
90	77.0	81.3	79.1	
95	61.8	70.8	65.0	76.6
100	52.2	62.1	54.3	64.5
105	49.9	60.5	51.5	60.1
110	43.3	53.6	45.2	52.9
114	42.1	52.9	41.9	50.2
120	35.5	45.0	37.3	45.3
125	34.0	43.6	32.0	38.8
130	31.9	41.2	29.0	35.4
135	30.4	39.2	26.6	32.4
140	27.4	35.1	22.5	29.5
145	27.4	32.3	20.1	25.7
150	24.0	29.6	17.8	22.3
155	22.2	26.8	16.3	20.9
160	19.7	23.6	15.0	19.1
165	18.5	21.6	14.2	16.9
170	16.0	20.1	13.3	17.2
175	15.0	18.2	12.8	
180	14.3	17.4	12.2	
α:	2.4	2.1	2.7	2.4

Since the angular dependence of the spectral shape is intimately related to the question of whether or not self-absorption is observable, a discussion of this aspect of the problem is necessary. A cathode ray electron (1) may be decelerated with the emission of a photon, or (2) may ionize an inner atomic level and eject a photoelectron. The excited state may disappear by a radiative or an Auger process. The photoelectrons, the Auger electrons as well as the Compton electrons will act as primary cathode ray electrons and give rise to a new cycle of events. Let P denote the probability that a photon of wavelength λ will be produced at a depth l by primary as well as secondary processes. P is a function of the electron energy at the distance l along the incident electron direction, the atomic number, and the emitted wavelength. The number of continuous x-ray photons emerging from unit area of the surface will depend on $\int_0^L P[E(l),\lambda,Z]e^{-\mu(\lambda)x}dl$, where $\mu(\lambda)$ is the linear absorption coefficient, x is the photon emergence length, and L is the maximum penetration depth as determined from electron range-energy investigations.[17]

The general formulation is not susceptible to numerical evaluation, but an estimate of the magnitude of the effect of self-absorption may be obtained from the simplified calculation which follows. If $C(\lambda)$ denotes the assumed constant rate of photon production per unit path length along l and emitted in the x direction (see Fig. 2), then $N(\lambda)$, the number of photons/sec of energy (hc/λ) which leave the target along the x direction from all points of l down to the depth L is given by

$$N(\lambda)=C(\lambda)\int_0^L e^{-\mu(\lambda)l\ \sec\theta}dl=C(\lambda)\frac{1-e^{-\mu(\lambda)L\ \sec\theta}}{\mu(\lambda)\ \sec\theta}. \quad (7)$$

In accordance with this model, a certain fraction $F(\lambda)$ of the total number of photons created will emerge from the surface. This fraction is

$$F(\lambda)=N(\lambda)/C(\lambda)L=(1-e^{-\xi})/\xi, \quad (8)$$

where $\xi=\mu(\lambda)L\sec\theta$. Typical values for L were calculated from the maximum range empirical relation given by Feldman[17] and are given in Table V. Linear absorption coefficients for magnesium and manganese have

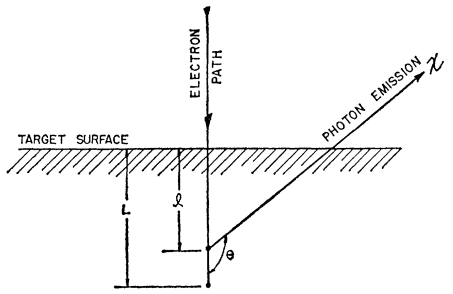

FIG. 2. Parameters involved in estimation of the effects of self-absorption.

[17] C. Feldman, Phys. Rev. **117**, 455 (1960).

TABLE V. Maximum ranges for low-energy electrons in Mg, Mn, and Ag.

Element	Magnesium		Manganese		Silver	
Energy in ev	675	1000	630	1200	1000	1500
Range in angstroms	200	390	29	110	28	73

been reported in this wavelength region[18,19] so that it was possible to calculate the values of $F(\lambda)$ for both Mg and Mn. In both cases, F was found to be essentially constant for $\theta\geqq 110°$. For $\theta=95°$, the calculations for Mg (0.675-kev run) showed a variation in F from 0.86 at $\lambda=100$ A to 0.79 at $\lambda=180$ A; and for Mn (1.2-kev run), $F(\lambda)$ ranged from a value of 0.49 at 80 A to 0.21 at 180 A. If $F(\lambda)$ is constant over the range of wavelengths considered, then it has no effect on the shape of observed distributions. Therefore it may be concluded that self-absorption represents a negligible correction to the spectra for $\theta\geqq 110°$. Application of $F(\lambda)$ to the data at $\theta=95°$ for Mg and Mn indicated that the long-wavelength intensities should be increased by 10% and 250%, respectively. Examination of the information given by Tables III and IV indicates no relative distortion of this magnitude. The simple model is deficient in that it ignores the degradation of electron energy with depth along with the details of the actual path of the electron. The ranges used for L are defined by Feldman to be the "maximum practical range"—that range beyond which no electrons could be experimentally detected. Upon entering the target, an electron undergoes many elastic and inelastic collisions with the result that its propagation is no longer rectilinear. Because of this straggling and energy degradation, only a small fraction of the incident electrons penetrate to depths approaching L. The average electron loses most of its initial energy in a volume whose depth is much smaller than that assumed in the model. Hence it is not surprising to see that the simplified model predicts excessive self-absorption effects at values of θ somewhat greater than 90°.

That self-absorption is negligible is also indicated by other observations. In the case of Mg, the observed absorption curve[18] shows that $\mu(\lambda)$ has a relatively narrow peak at 155 A, but the continuum shows no corresponding modification in shape which is indicative of the effects of this change in the behavior of $\mu(\lambda)$. For Mn, a pronounced narrow minimum in $\mu(\lambda)$ is reported[19] at 165 A, but all the Mn emission spectra show a smooth monotonically decreasing intensity from $\lambda=140$ A to $\lambda=180$ A.

4. Comparison with Theory—Mg and Mn

The calculations of Kirkpatrick and Weidmann cover the range $0.00985\leqq V/Z^2\leqq 1.776$ statvolts and

[18] J. R. Townsend, Phys. Rev. **92**, 556 (1953).
[19] D. H. Tomboulian, D. E. Bedo, and W. M. Neupert, J. Phys. Chem. Solids **3**, 282 (1957).

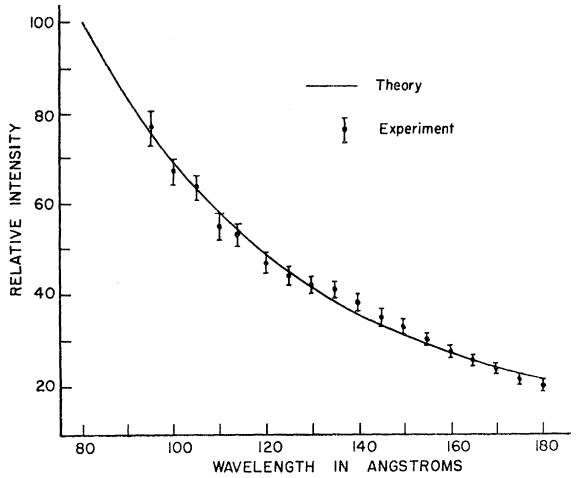

FIG. 3. Comparison of theory with observation. Mn target at 630 v and at a takeoff angle of 95°. The experimental error is denoted by vertical bars.

provide readily useable intensity results for $\nu/\nu_0>0.1$. This latter condition requires that the accelerating voltages be kept below 700 v. At potentials of this magnitude, screening of the nucleus by the electron cloud must be taken into account, as the calculations are based on the assumption that the electron "sees" the unshielded entire nuclear charge. The accelerating potential of 675 v used for Mg is considerably less than the K ionization potential (1300 v); thus the nuclear charge is screened to some degree. The error made by using $Z=12$ for Mg is of the order of 2 units of nuclear charge; therefore the calculations were made using $Z=10$. The predictions from theory and observations may be compared by referring to Fig. 1 and the data in Table III.

The Kirkpatrick and Wiedmann calculations included screening for the long-wavelength portions of the spectrum and they used the screened potential function

$$V=-(eZ/r)e^{-r/a}, \tag{9}$$

where r is measured from the nucleus and a is a parameter depending only on Z. They report $a=0.5$ A as a suitable choice for Mn. Slater[20] has tabulated the distance at which the radial charge densities of atoms are greatest, giving 0.42 A for Mn $3d$ and 1.31 A for Mn $4s$ electrons. In the light of the above we can then use Slater's empirical screening constants[21] to find Z as if the electron were always interacting with the field as seen by a $3d$ electron in Mn. Application of the Slater constants gives an effective $Z=14.55$ and with $V=630$ v this gives $V/Z^2=0.00992$ statvolt. In the case of Mn, this was the value used to obtain the magnitudes of the intensity components I_x and I_y.

[20] J. C. Slater, *Introduction to Chemical Physics* (McGraw-Hill Book Company, New York, 1939), 1st ed., p. 349.
[21] J. C. Slater, Phys. Rev. **36**, 57 (1930).

TABLE VI. Theoretical and experimental values of $I(\lambda)$ from a Mn target at 630 v and a takeoff angle of 95°.

Wavelength in angstroms	Relative intensities	
	Theory	Experiment
80	100	
85	91.0	
90	82.6	
95	75.5	76.6
100	69.2	67.2
105	63.2	63.5
110	58.0	55.0
114	54.2	53.3
120	48.7	47.0
125	45.0	44.0
130	41.5	42.2
135	38.3	41.0
140	35.5	38.4
145	33.2	34.9
150	30.9	33.1
155	29.0	30.3
160	27.2	27.4
165	25.6	25.7
170	24.1	23.4
175	22.7	21.1
180	21.4	19.6

For a comparison of theory with experiment see Fig. 3 and Table VI.

The satisfactory agreement between the somewhat idealized theory and the present results can be more easily understood with the help of additional results from Kirkpatrick and Wiedmann.[9] Figure 4 gives relative intensity plots for accelerating potentials of 675 v, 500 v, and 295 v in the case of $Z=10$. The curves indicate that the spectrum from electrons having lost even more than half their energy is not significantly different from the spectrum predicted under the assumption that all the radiating electrons have the same maximum kinetic energy at the time of interaction. Since the electrons are brought to rest in the target layer, it follows that radiation is emitted by electrons with kinetic energies lower than that acquired

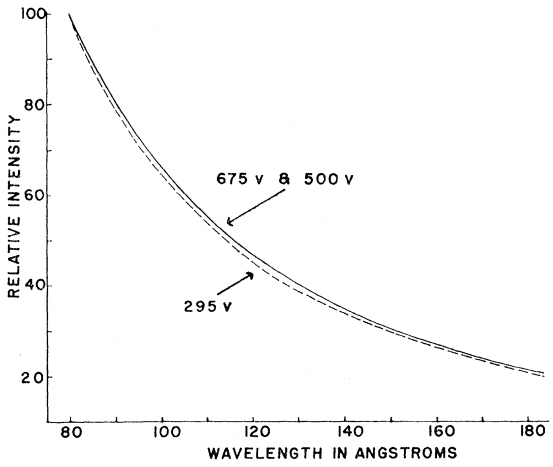

FIG. 4. Predicted intensities using $Z=10$ and at the indicated voltages.

from the accelerating potential. In the absence of self-absorption, the curves of Fig. 4 indicate that the spectra from a thin target and a thick target should have essentially the same energy distribution *if* the significant portion of the radiation is contributed by electrons having lost less than 60% of their initial kinetic energy, and *if* the wavelength range of observed radiation is far removed from the Duane-Hunt limit as is the case in the present work.

IV. CONCLUDING REMARKS

The present paper is a report of a pioneering investigation of the continuous x-ray spectrum which was made possible by the availability of a calibrated spectrograph.

It may be stated that for incident electrons in the 500-ev to 3000-ev energy range, the observed intensity per unit wavelength interval in the soft x-ray continuous spectrum is not proportional to $1/\lambda^2$, but it can be represented over a moderate wavelength interval by $1/\lambda^\alpha$. It is found that $1.8<\alpha<2.7$, where α is a parameter which is intimately related to the accelerating potential, the Z of the target, and the ν/ν_0 range of observation.

Furthermore, the observed spectral distribution is dependent to some extent upon the angle of observation. The available information indicates that this variation is not a result of self-absorption within the target, but rather it is a manifestation of ideal thin-target behavior. This appearance of dependence on angle is in accord with other results[22] obtained at higher potentials (6 to 12 kev) where, again, electron-opaque targets show traces of thin target behavior. The usable calculated results limit comparison between theory and experiment; however, in all cases studied, the effect of changes in the takeoff angle proved to be in qualitative harmony.

The observations on Mg and Mn are quite consistent with the predictions that the spectral shape over the 80–180 A wavelength span should be relatively insensitive to electron energy losses in body of the target. Insofar as the choice of Z in determining a value of V/Z^2 is concerned, the approximation method used for Mn is admittedly crude, but it is also a reflection of knowledge that the relative intensities for very low V are insensitive to small changes in Z.

ACKNOWLEDGMENTS

The authors are indebted to Professor E. E. Salpeter for helpful comments. We also thank Mr. L. H. Hinman for technical assistance in construction of the x-ray tube.

[22] N. A. Dyson, Proc. Phys. Soc. (London) **73**, 924 (1959).